Universiteit
Leiden
The Netherlands

Lighting up cancer aggressiveness: targeting the urokinase plasminogen activator receptor for intraoperative optical imaging

Baart, V.M.

Citation
Baart, V. M. (2023, December 14). *Lighting up cancer aggressiveness: targeting the urokinase plasminogen activator receptor for intraoperative optical imaging*. Retrieved from https://hdl.handle.net/1887/3673489

Version:	Publisher's Version
License:	Licence agreement concerning inclusion of doctoral thesis in the Institutional Repository of the University of Leiden
Downloaded from:	https://hdl.handle.net/1887/3673489

Note: To cite this publication please use the final published version (if applicable).

Chapter 9

General discussion and future perspectives

Baart VM

General discussion and future perspectives

In merely a decade the targeted-fluorescence guided surgery (FGS) field has made significant strides forward, from the initial proof-of-concept trial by van Dam et al. in 2011 to the in 2021 United States Food and Drug Administration approval of the first targeted near-infrared (NIR) fluorescence contrast agent pafolacianine (Cytalux; i.e. OTL38) [1]. FGS has matured from promises of clinical benefit to demonstrating the applicability in a randomized phase III-trial; pafolacianine identified 33% additional lesions in ovarian cancer patients that otherwise would have been missed by the operating surgeon [2]. As more phase-III trials with other agents are expected to report their outcomes in the upcoming years, the surgical scientific community stands at the footsteps of an era of precision surgery, where tumors can be color-coded to aid intraoperative decision making and resection [3].

Fundamental for a fluorescent tracer is the framework of clinical application applied and whether the desired contrast is achieved. For example, 40% of ovarian cancer patients show residual lesions larger than 1 cm by postoperative computed tomography after cytoreductive complete resection. Subsequently this group had inferior outcomes compared to patients where intraoperative assessment was in accordance with postoperative imaging [4]. The NIR contrast agent pafolacianine can play a role into this clinical framework, by offering an innovative approach to identify and resect these missed lesions intraoperatively. For this purpose pafolacianine has been improved upon its predecessor EC17 by utilizing the NIR window as opposed to blue light. This exchange of fluorophore enhances the contrast by decreasing background autofluorescence and improving penetration depth of the signal [1, 5]. While the steps being made are exciting, the pafolacianine FDA approval also obliges us to ask what the next-generation of FGS contrast agents will look like and particularly whether there is room for urokinase plasminogen activator receptor (uPAR)-targeted FGS in this landscape.

The following section will therefore discuss (I) the clinical frameworks where FGS could be of clinical value, (II) where uPAR fits in these clinical frameworks, (III) how tumor contrast can be enhanced by smart tracer design.

Part I. Clinical frameworks for FGS

As the possibilities with FGS broaden, it becomes paramount to focus on the clinical frameworks where FGS can potentially enhance patient survival by improving surgical outcomes [6]. Based on the current literature, Table 1 identifies fourteen clinical questions for eleven solid tumor types where FGS offers a potential application. While one question addresses staging by identifying radiographically occult lesions and two focus on identifying additional lesions during debulking procedures, the majority (11) focus on improving locoregional tumor control by improving R0 resection margin rates. Especially in (potentially) locally advanced tumors, such as those in the head & neck, brain or rectum, margin positivity rates are high and the potential of additional intraoperative guidance via FGS is obvious [7-9].

After defining the clinical framework potential targets need to be assessed. Identifying a target expressed across all tumors and absent in non-malignant tissue, comprising normal, benign and reactive tissue like inflamed or fibrotic, is the holy grail of molecular imaging modalities including FGS. Finding such a target, however, is nearly impossible as cancer is an umbrella term for more than 100 diseases that fails to highlight the inter-tumoral heterogeneity that exists, even between tumors from similar anatomical origins[1] [10, 11]. Not surprisingly, the twenty FGS-tracers that are undergoing clinical translation target fifteen different proteins or processes [3]. In Table 1 potential targets are identified for the FGS clinical frameworks mentioned above, based on (pre-) clinical data and stage of development[2]. While the folate receptor is specific for ovarian cancer, carcinoembryonic antigen (CEA) for gastro-intestinal tumors, and epidermal growth factor receptor (EGFR) for head & neck cancer, uPAR's versatility as potential target for head & neck, pancreatic, ovarian, prostate, and bladder cancer suggests merits as a next-generation target.

1 Intra-tumoral heterogeneity complicates matters even further when subclones in the tumor decrease or eliminate the expression of the target.

2 The list of potential targets is meant to be exemplary and is not an exhaustive list.

Table 1. Possible clinical frameworks where FGS is a potential solution to improve surgical outcomes and relevant targets.

Tumor Type	Clinical Framework	Framework type	Potential targets[#]
Glioma	Increasing percentage of patients with maximal cytoreductive surgery by improving visualization of the infiltrative zone (≈65% [8])	Locoregional control	Protoporphyrin IX precursors; **uPAR**
Head & neck cancer	Reducing tumor-positive margins of head & neck squamous cell carcinoma patients treated by resection (≈ 23.3% [7])	Locoregional control	Integrin αvß6; EGFR; **uPAR**
Breast cancer	Improving re-excision rates of breast cancer patients treated by lumpectomy (≈ 21.6% [12])	Locoregional control	Cathepsin/ proteolytic activity
Lung	Reducing positive resection margins (5-15% [13])	Locoregional control	Non-targeted; folate receptor; CAIX; Collagen XVII
Esophageal cancer	Reducing margin positivity rate in patients with esophageal cancer undergoing an esophagectomy (≈ 9.4% [14])	Locoregional control	EpCAM; CEA
Primary and secondary liver cancer	Reducing tumor-positive margins of primary and secondary hepatic lesions (≈ 28% tumor-positive margins for colorectal liver metastases [15])	Locoregional control	Non-targeted; CEA
Pancreatic cancer	Preventing unnecessary laparotomies in patients with pancreatic ductal adenocarcinoma by detecting radiographically occult disease during the staging laparoscopy (≈ 20% have unresectable disease during laparotomy [16])	Staging	Integrin αvß6; CEA; **uPAR**
	Reducing R1 positive margins in patients with pancreatic ductal adenocarcinoma undergoing laparotomy with curative intent (≈ 50-70% [17])	Locoregional control	
Colorectal	Improving cytoreductive resections in patients with peritoneal carcinomatosis of colorectal origin [18]	Identifying additional lesions	CEA; EpCAM
	Reducing R1 resection margins in patients with locally advanced rectal cancer (≈ 16% [9])	Locoregional control	
Ovarian	Improving detection of subclinical peritoneal nodules in staging and debulking procedures for patients with epithelial ovarian carcinoma [6]	Identifying additional lesions	Folate receptor; **uPAR**; EpCAM
Prostate	Reducing positive margins during in patients undergoing radical prostatectomy (≈ 15% [19])	Locoregional control	PSMA; **uPAR**
Bladder	Reducing recurrence rates in patients with non-muscle invasive bladder cancer (30-80% [20])	Locoregional control	Protoporphyrin IX precursors; **uPAR**
	Reducing positive soft tissue surgical margins in patients undergoing radical cystectomy for primary urothelial cancer (≈ 4.2% [21])	Locoregional control	

targets are identified based on available (pre-)clinical data and stage of development. The list is not meant to be exhaustive. See Table 2 and 3 for in-depth evidence supporting the targets relevance. CAIX, carbonic anhydrase IX; CEA, carcinoembryonic antigen; EGFR, epidermal growth factor receptor; EpCAM, epithelial cell adhesion molecule; PSMA, prostate-specific membrane antigen; uPAR, urokinase plasminogen activator receptor.

Part II. Clinical framework of uPAR-based FGS

Biology of uPAR

Understanding the complex biology of uPAR helps to explain its versatility as a target. Mechanistically, uPAR can be considered a lynchpin protein or central orchestrator in many of the pathways fundamental to cancer. Proteomic studies, for instance, show that a moderate downregulation of uPAR (approx. 43%) reverses signaling pathways associated with eight of the ten defined 'Hallmarks of Cancer', most importantly those involving the evasion of cancer cell death, promoting cancer cell proliferation, activating invasion and metastases, and promoting immune evasion [22-26]. *In vitro* and *in vivo* studies confirm many of these associations and show uPAR to be closely related to tumor-aggressiveness [27]. Because of the universal characteristics uPAR seems a marker for cancer biology rather than a marker for specific cancer types.

Not surprisingly, uPAR (over-)expression has been described in almost every solid malignancy and expression is often correlated with poor prognosis [27-29]. We confirm this pattern for pancreatic ductal adenocarcinoma in **Chapter 2**,where uPAR expression in both neoplastic and stromal cells is inversely associated with overall survival (OS) and disease-free survival (DFS) of the patients. Similarly, we show in **Chapter 3,** that uPAR is overexpressed in the majority of squamous cell carcinoma's of the head and neck, again on both neoplastic and tumor-associated stromal cells, whereas adjacent normal tissue contained no uPAR expression. The results from this study are especially relevant for FGS as tissue samples were specifically selected and evaluated based on the presence of tumor margins. As such, this studies builds on the evidence that uPAR expression particularly localizes towards the invasive edge, often the margin at risk during surgical resection [30].

Clinical experience with uPAR

uPAR's pathophysiological role in tumor progression and the association with DFS and OS in numerous solid tumor types make it an established prognostic target and potential aid in treatment stratification. Not surprisingly, the first phase II clinical trial demonstrating molecular imaging of uPAR was focused down this avenue: Fosbøl et al. have been able to discriminate prostate cancer patients in low-risk and intermediate-risk Gleason score based on standardized uptake values (SUV) of the uPAR targeting positron emission tomography (PET) ligand ^{68}Ga-NOTA-AE105 [31]. Similarly, in two different phase II clinical trials relapse-free survival has been predicted in patients with head and neck squamous cell carcinoma, and prognosis has been associated with uPAR in patients with neuroendocrine neoplasms using the same tracer [32, 33]. A fourth phase II clinical trial in patients with metastatic

castration-resistant prostate cancer undergoing radium-223 therapy had to be prematurely terminated because of inclusion challenges due to changes in treatment guidelines. However the acquired data showed an association between SUV_{max} of the index lesion and OS [34]. As the road has been paved for uPAR-based PET, it might be time for uPAR-based FGS to follow.

uPAR-based FGS

The clinical framework within which uPAR FGS has the most potential focusses on patient-groups where tumor margins are narrow and most at risk as uPAR's upregulation is often most prominent at the (invasive) tumor-stromal interface [30, 35]. For instance, irradical resection rates can be up to 60% for high risk squamous cell carcinomas of the head & neck (HNSSC) and are directly associated with poor patient outcomes. As uPAR is (over-) expressed in the majority of HNSSC patients (up to 100% of patients), uPAR FGS in the complicated head & neck surgical landscape is a promising avenue to lower irradical resection rates [29, 36, 37]. A similar case could be made for malignant gliomas, where maximal cytoreductive surgery is an essential part in the treatment process, but where it is achieved in less than 35% of cases without additional imaging and in 65% of patients with 5-aminolevulinic acid based intraoperative imaging [8, 38]. As uPAR is (over-)expressed in the majority of glioma's, targeting uPAR for FGS could potentially improve the negative margin rates [39-41].

Recently, FluoGuide, a clinical stage biotechnology company focused on FGS that is translating a uPAR targeting fluorescent peptide towards the clinic, confirmed the uPAR approach by reporting a first-in-human study using the uPAR targeting peptide FG001 (AE105-Glu-Glu-ICG) for the visualization of malignant gliomas. In this open-label, non-randomized, dose-escalation phase I/IIa study FG001 was deemed safe and resulted in TBRs of approximately 2.3 (1.8-2.6) with the Orbeye camera system and 3.5 (2.8-4.6) with the Zeiss Pentero C camera system. The specificity, sensitivity, positive-predictive value and negative-predictive value were 100% (59-100%), 79% (58-93%), 100% (82-100%) and 58% (28-85%), respectively [42]. Based on these results, FluoGuide has commenced with phase IIb studies in high grade glioma patients and initiated phase IIa trials in patients with lung cancer and head & neck cancer (EudraCT number 2022-0013612-12, 2021-004389-37).

uPAR FGS compared to other targets

uPAR is a versatile target that has, as outlined above, potential as FGS target for various tumor types where local tumor margins are at risk. Obviously, uPAR is not the only target that is being studied. The key question is how uPAR performs compared to other targets for the clinical frameworks previously identified?

Although alternative targets exists, adequately comparing targets is challenging. The literature that exists is mostly based on immunohistochemical (IHC) methods, and studies comparing targets in *in vivo* or clinical settings are practically non-existent[43-48]. Therefore, it is important to be aware of the biases and/or limitations of IHC studies. First-of-all, as Ahn et al. so eloquently demonstrated using different monoclonal antibodies targeting the same receptor can result in two very contrasting expression patterns [49]. Secondly, the tissue origin is of utmost important as Serpa et al. show that expression patterns differs significantly between location: 76.7% of cases were positive at the invasion front but only 48.4% at the tumor core [50]. Lastly, studies differ in scoring systems and what accounts a positive score. A close look needs to be taken whether only epithelial cells are scored or also the stromal compartment, and what percentage of cells should show expression for a positive expression score.

Despite the limitations, Table 2 compares the expression pattern of uPAR with other promising targets for the uPAR clinical frameworks identified earlier. For most indications alternative targets can be found with similar expression rates on tumor tissue. However, unlike uPAR[3], these alternatives often have significant expression in normal tissue, potentially increasing background fluorescence [30]. For example, as identified in **Chapter 3,** both integrin $\alpha_v ß_6$ and EGFR are weakly to highly expressed on normal squamous epithelium, whereas uPAR is absent. Furthermore, another advantage of uPAR is that it is also expressed on the tumor-associated stromal compartment whereas integrin $\alpha_v ß_6$, EGFR, CEA, EpCAM, and prostate-specific membrane antigen (PSMA) are solely expressed on the tumor compartment [49-51]. The challenge, however, with targeting uPAR is its heterogenous pattern of expression. Whether this heterogeneity is relevant, as high uPAR is often expressed at FGS sites like tumor border, or impairing like less prominent presence in tumor cores, remains to be evaluated [50]. Table 3 compares targets for the clinical frameworks where uPAR has less potential.

3 In normal tissue, uPAR expression is mostly limited to bone-marrow derived white blood cells, pulmonary alveoli, glomeruli and a sporadic endothelial cell. In healthy individuals, uPAR is not critical for normal physiology. uPAR becomes upregulated in tissues undergoing active remodeling such as during wound-healing, embryo implantation or mammary gland involution [29].

Table 2. Comparison of uPAR to other potential targets for the clinical frameworks where uPAR has been identified as being promising.

Target	Potential Tracer	Remarks
Glioma		
uPAR	FG001 *FG002* *huATN658-IRDye800CW** *huNb2-IRDye800CW*	⊕ 95% elevated uPAR expression [41] ⊕ Specificity 79%, Sensitivity 100%, PPV 100%, NPV 58% [42] ⊕ Average TBR 2.3-3.5 [42] ⊕/⊖ Heterogenous staining pattern [40]
Chlorotoxin derived peptide	BLZ-100	⊕ 6/6 (100%) high-grade tumors fluorescence [52] ⊕/⊖ Unclear binding mechanism [52]
EGFR	Cetuximab-IRDye800CW Panitumumab-IRDye800CW ABY-029	⊕ Overexpressed in 54-80% of patients [53-55] ⊕ Expression decreased in normal brain tissue [56] ⊕ TBR 4.0 ± 0.5 [56]
Head & neck cancer		
uPAR	See above	⊕ Expressed in 64-100% of primary tumors [36, 37, 57] ⊕ Expressed on both tumor and tumor-surrounding stromal cells [36, 37, 57] ⊕ Absent on normal squamous epithelium and adnexa [36, 37, 57] ⊕/⊖ Expression can be heterogenous [36, 37]
Integrin $\alpha_v ß_6$	*R01-MG-IRDye800CW**	⊕ Expressed in 87-95% of primary tumors [36, 58] ⊕/⊖ Low to moderate expression on normal squamous epithelium and adnexa [36, 58]
EGFR	See above	⊕ Expressed in 100% of primary tumors [36, 37] ⊖ High expression on normal squamous epithelium and adnexa [36, 37]
Pancreatic cancer		
uPAR	See above	⊕ Expressed in 67-82% of patients [43, 59] ⊕ Significantly overexpressed compared to chronic pancreatitis [44] ⊕ Expressed on both tumor and tumor-surrounding stromal cells [44, 59] ⊕ Complete absence of staining in normal pancreatic tissue [44] ⊖ High uPAR expression in negative lymph nodes [44]
Integrin $\alpha_v ß_6$	See above	⊕ Highly expressed in 88% patients [43] ⊕ Sensitivity of 84% and specificity of 100% for tumor lymph nodes [44] ⊕ Significantly overexpressed compared to chronic pancreatitis ⊖ Moderate staining in normal ductal structures [44]
CEA	SGM-101	⊕ Highly expressed in 71% of patients [43] ⊕ Completely absent in normal pancreatic parenchyma [44] ⊕ Significantly overexpressed compared to chronic pancreatitis ⊕ Sensitivity of 68% and specificity of 100% for tumor lymph nodes [44] ⊖ Heterogenous expression and loss of expression after neoadjuvant treatment [44]

Table 2. Continued.

Target	Potential Tracer	Remarks
Ovarian cancer		
uPAR	See above	⊕ Expressed in >80% of patients in 7/9 studies [60] ⊕ Expression independent of histology [60] ⊕ Expressed predominantly on tumor cells but also on tumor-surrounding stromal cells [60] ⊕ Expression low to absent on benign tissue [60] ⊕ No difference in expression between primary and metastatic lesions [60]
Folate-receptor	OTL38	⊕ Overexpressed in 72-97% of patients [61, 62] ⊕Additional lesions not detected by white light in 33% of patients [63] ⊕ Sensitivity 83% (0.74-0.89) [63] ⊖ Lesion false-positive 32.7% [63]
EpCAM	*R01-MG-IRDye800CW*	⊕ Overexpressed in 78-88% of lesions [64, 65] ⊕ Sensitivity 88%, specificity 100%, PPV 100%, NPV 94% for tumor-positive lymph nodes [65] ⊕/⊖ Overexpression rate dependent of histology [64] ⊖ Low to high expression on normal epithelium of the digestive tract [66]
Prostate		
uPAR	See above	⊕ Overexpressed in 64% of primary tissue and in >90% of lymph node metastases [67] ⊕ Not expressed in normal prostate or benign tissue [67, 68] ⊕ Expressed on tumor associated stromal cells [67, 68] ⊖ Expression can be heterogenous [67, 68]
PSMA	*OTL78*	⊕ Expressed in 80-96% of primary tumors and 84% of metastases [69, 70] ⊕/⊖ Expressed in the small intestine, proximal renal tubules, and salivary and lacrimal glands [71] ⊖ Expressed in normal prostate epithelium [71]
Bladder		
uPAR	See above	⊕ Expressed on 96% of tumors [72] ⊕ Expressed particularly at the invasive front [72] ⊕ Expression independent of grade and stage [72] ⊕ Expressed on tumor associated stromal cells [72] ⊕ Absent in normal bladder epithelium [72, 73] ⊕/⊖ Expression can be heterogenous [73]
Protoporphyrin IX precursors	HAL 5-ALA	⊕ Relative reduction of 16-20% (56 vs. 47%; $p<0.026$) in recurrence after transurethral resection [73, 74] ⊕ 7-32% additional patients identified ($p<0.0001$) [73, 74] ⊕ Intravesical application [74] ⊖ Not suitable for radical cystectomy

* tracers in italics are in preclinical development stage

Table 3. Comparison of potential FGS targets and their tracers, where uPAR has less potential

Target	Potential Tracer	Remarks
Lung		
Non-targeted	ICG	⊕ Sensitivity 86.4-89.3%, 11.8-18.2 false-positive [77] ⊕ Detects additional lesions (9/14 malignant) [77] ⊖ 9.1-13% false negative [77]
Folate receptor	OTL38	⊕ 72-87% of lung adenocarcinomas [77] ⊖ 13-57% of lung squamous cell carcinomas [77] ⊕ Sensitivity 84% in adenocarcinomas and 58% in squamous cell carcinomas [78, 79] ⊕ 56.3-100% of fluorescent margins true positives [80-82] ⊖ No difference in TBR between malignant and benign lesions [83]
Breast cancer		
Cathepsin activity	LUM015	⊕ Adequate fluorescence for tumor detection in 87-100% of patients [84, 85] ⊕ Signal not dependent on tumor subtype ⊕ Specificity 73% [84, 85] ⊕ Sensitivity for residual tumor detection 100% [84, 85]
Proteolytic activity	AVB-620	⊕ Signal not dependent on tumor subtype [86] ⊕ Specificity 78% [86] ⊕ Lumpectomy re-excision rate 6% as opposed to 20-40% [86] ⊕ 75% additional positive margins detected [86]
Esophagus		
EpCAM	*VB5-845D-800CW**	⊕ Expressed in 98% - 100% of primary tumors [87, 88] ⊕ Expressed in 100% of residual tumor tissue after neoadjuvant chemoradiotherapy [87] ⊕ Tumor-to-normal ratio >10 [87] ⊕/⊖ Low to moderate expression in normal epithelial tissue [87, 88]
CEA	SGM-101	⊕ Tumor-to-normal ratio 3.62 [87] ⊕/⊖ Expressed in 54% of primary tumors [87] ⊕/⊖ Low to moderate expression in normal epithelial tissue [87]
Primary and secondary liver cancer		
Non-targeted	ICG	⊕ Suitable for all primary and secondary liver lesions [89, 90] ⊕ Tumor negative margins in 88% of lesions with no fluorescence in wound bed vs. 0% of lesions with fluorescence in wound bed [91]
CEA	SGM-101	⊕/⊖ Suitable for secondary liver lesions where the primary is known to express CEA (i.e. colorectal and pancreatic metastases → 89% true positive) [92]
Colorectal		
CEA	SGM-101	⊕ Overexpressed in 98.8% of tumors compared to matched normal tissue [93] ⊕ Expression on healthy tissue is on average 60 times lower [11] ⊕ CEA expression is not altered after chemoradiotherapy [94]
EpCAM	*VB5-845D-800CW*	⊕ Overexpressed in 94-97.7% of tumors [64, 94, 95] ⊕ EpCAM expression is not altered after chemoradiotherapy [94] ⊕/⊖ EpCAM is also expressed in normal tissue [96]

* tracers in italics are in preclinical development stage

uPAR FGS indications beyond oncology

uPAR expression is not unique to cancer and, as elaborated on in **Chapter 4**, uPAR plays a relevant pathophysiological role in a multitude of other diseases, including atherosclerosis, rheumatoid arthritis (RA), Alzheimer's disease, multiple sclerosis, and inflammatory bowel disease. There are currently no clear indications

for uPAR FGS beyond oncology. However, there are a couple avenues to explore where uPAR non-invasive molecular imaging deserves further exploration. Just recently, in a proof-of-concept retrospective analysis study, Khare et al. were able to clinically visualize heterogenous uptake of [^{64}Cu]Cu-DOTA-AE105 on PET/CT in atherosclerotic lesions of the large conductive arteries of ten cancer patients enrolled in the phase I clinical trial of the respective tracer [75]. While this study suggests the feasibility of atherosclerotic imaging via uPAR, further properly powered studies will need to demonstrate the clinically utility. Another potential avenue worth exploring is that of therapy (de-) escalation of RA. uPAR plays an essential role in disease pathophysiology and RA activity is correlated with plasma levels of soluble uPAR, derived from uPAR expressing cells [76]. A rather simple urine or plasma ELISA for uPAR could aid clinicians in proper managing of RA. Compared to cancer, our understanding of uPAR in these various diseases is limited[4] and as our understanding expands, additional diagnostic, prognostic, and therapeutic opportunities will present themselves.

Part III. Enhancing tumor contrast by smart tracer design

The primary aim of a molecular imaging tracer is delivering the NIR fluorescent agent to the target site. Rapid clearance from irrelevant sites is therefor of key importance to achieve high contrasts between the target site and the adjacent tissue. Characteristics, such as molecular weight, affinity, 3D confirmation, charge, and conjugation method of the tracer play a pivotal role in creating this contrast as these characteristics play a determining factor in tracer distribution and kinetics. Therefore, in **Chapters 5-8** exceedingly smaller antibody-based uPAR targeting tracers have been developed in order to identify the most appropriate construct for FGS to apply into the clinic. This intermezzo is not specific for uPAR but explains basic characteristics of tracer design which are employed in **Chapters 6-8**.

4 A PubMed search on "uPAR" and "Cancer" yields more than 1700 entries while searches on "uPAR" and "atherosclerosis", "uPAR" and "rheumatoid arthritis", "uPAR" and "Alzheimer", "uPAR" and "multiple sclerosis", and "uPAR" and "inflammatory bowel disease" result in 68, 27, 13, 10 and 7 results respectively. Date of search: July 2022.

The influence of molecular weight on tumor signal

There exists an inverted bell-shaped trade-off between molecular weight and tumor accumulation when comparing molecular imaging tracers with similar target affinities [97]. Underlying variables, amongst others, of this relationship are tracer diffusion/extravasation (i.e. tumor uptake) and clearance (i.e. tracer removal). Diffusion is the net movement of molecules from regions of high concentration to regions of low concentration and the speed of this is inversely proportional to the molecular radius [98]. Therefore, smaller tracers such as $F(ab')_2$s (≈110 kDa), Fabs (≈55kDa) and VHHs (≈15kDa) are expected to diffuse more rapidly into tissue than full-sized antibodies (≈150kDa). Where improving diffusion stimulates tumor uptake, improving clearance reduces this. Clearance can be modulated by decreasing molecular weight, so that tracers fall below the size cut-off for glomerular filtration by the kidneys, estimated between 30-50 kDa, and by removing Fc-domains so that Fc receptor-mediated recycling is bypassed [99]. Importantly, in modeling and *in vivo* studies there exists an impasse around 25-50 kDa, where the improved diffusion offered by decrease in tracer radius is not compensated in proportion for the rapid renal clearance that starts occurring at this molecular weight, resulting in lower signal intensities than tracers with larger or smaller molecular weights [100-107].

The influence of affinity on tumor signal

Where molecular weight influences tumor uptake and clearance from the circulation, affinity keeps a tracer in the tumor. Improving affinity, up to a plateau level (for antibodies around 10n*M* K_d), improves signal intensity linearly[5]. This plateau level increases with decreasing molecular size [108-112]. High affinities are especially relevant for small compounds, such as peptides, as their rapid diffusion into the tumor also means they rapidly diffuse out of the tumor. Therefore relatively small peptides are dependent on high affinities to be retained. Modelling studies show that peptides need approximately a hundred-fold higher affinity to keep them anchored to the tumor and achieve similar signal intensities than the much larger monoclonal antibodies [97].

The influence of conjugation method on tumor signal

Next to molecular weight and affinity, the method of conjugating the contrast agent with the tracer is a third component that can influence imaging results dramatically.

5 It is relevant to realize that while improving affinity above the threshold might not improve tracer accumulation there can be other effects achieved with higher affinities. For instance, in the case of antibody-directed cellular cytotoxicity higher affinities do result in more effective treatment [35].

Conjugation can be either non-specific (free amine-groups) or site-specific. While the former is both rapid and easy, it results in heterogenous products with potential modifications on or near complementarity-determining regions potentially altering binding affinity and specificity [113]. This random effect increases with the degree-of-labelling (DoL) and defining a DoL that balances fluorescence intensity and potential pharmacokinetic effects (increased clearance, increased liver uptake) is crucial. Current studies set the optimal DoL around 0.3 - 2.0 for antibodies[6] [114-116]. The alternative, site-specific labelling, ensures a more homogenous end-product with superior plasma stability, binding efficiency, and tumor uptake [113]. This effect is more pronounced for smaller antibody-based compounds where, for example, non-site-specific labelled nanobodies resulted in a lack of specific tumor signal at a DoL of 1.1 – 1.4 compared to site-specific labelled nanobodies with a DoL of 1.0 [117]. Disadvantages for site-specific conjugation are the more challenging purification methods needed and potential of 3D-damage to the tracer. Peptides are in principle always site specifically labelled.

The influence of tracer design on logistics

An important last argument, especially for advocates of smaller tracers such as peptides and nanobodies, is the clinical logistics, as their rapid clearance allows same-day imaging [118, 119]. In FGS clinical trials, antibodies and even tracers as small as Fabs have to be administered 3-5 days prior to surgery in order to achieve adequate fluorescence contrast between target sites and the background, while the much smaller peptides can be administered the same day, minutes to hours before surgery [5, 120, 121]. Practically this difference translates to patients being burdened with an additional hospital visit when receiving tracers that are not amendable to same-day imaging [118]. The production also differs between antibody-based productions and peptides. The latter are made in non-biological systems resulting in possible favorable safety profiles and lower production costs [122]. It should be clear that while optimizing patient experience and keeping costs low is important, logistics should not be the deciding factor, unless two tracers clinically give similar results.

6 Non-site specific labelling follows a Poisson distribution. *In vivo*, fluorescence, however, is skewed towards antibodies with several dyes as antibodies with no dyes are not fluorescent and antibodies with two or more dyes are approximately twice as fluorescent (or more). At an DoL of 1.2 70% of the fluorescence comes from antibodies with 2 or more dyes [47]. Therefore, over-labelling is a serious issue that influences signal specificity. Our group aims for a DoL of 0.9 – 1.5.

Identifying optimal tracer characteristics

In conclusion, selecting optimal tracer characteristics for FGS requires, amongst others, balancing molecular weight, affinity and conjugation methods. First-of-all, site-specific conjugation is preferred for all tracers and essential for smaller tracers. Secondly, higher affinities are more crucial for smaller tracers than larger ones. Thirdly, a molecular weight between 20-50kDa should be avoided as this range leads to inferior signal intensities compared to tracers that are larger or smaller. Logistics and production costs can play a further role in identifying the optimal tracer by categorizing tracers into two groups: same-day vs. different-day imaging. Tracers larger than 20-50kDa fall into the different-day imaging. Here, in vivo comparative studies show higher peak tumor fluorescence for antibodies than their constructs, a quality that is imperative in identifying smaller tumor lesions, and therefore have an advantage. There is practically no data comparing different tracers < 20kDa and therefore an ideal construct in the same-day imaging category is hard to identify.

In **Chapters 6-7** an uPAR targeting monoclonal antibody, F(ab')2, and Fab, were introduced *in vivo* (Figure 1A). The major difference between these structures was their molecular weight, as their affinities for uPAR were equal or similar and labelling methods were the same. The difference in molecular weight (molecular weights: IgG, 150kDa; F(ab')2, 110kDa; Fab, 55kDa) lead to differing absolute tumor signal (Figure 1B). It was highest for the monoclonal antibody and it was significantly lower for the F(ab')2 and Fab. While a high absolute signal improves sensitivity, ultimately, a clear contrast between tumor and background tissue is needed for accurate intraoperative visualization. This is contrast is generally reported as the tumor-to-background ratio (TBR), where a ratio higher than 1.5 is deemed permissible and above 2.0 preferred [123]. TBRs did not differ between the tracers. Furthermore, the ideal imaging window differed between the tracers where tumors could be imaged within 24hrs for the Fab, 36hrs for the F(ab')2 and 72hrs for the full-sized antibody. In this comparison, the monoclonal antibody is the most ideal candidates to develop into clinical constructs as it results in the best imaging at the expense of larger imaging window.

How do the uPAR targeting tracers developed in this thesis compare to the uPAR targeting peptide AE105-Glu-Glu-ICG currently in clinical trials? In terms of imaging characteristics AE105-Glu-Glu-ICG has a rapid imaging window allowing same-day imaging and reported TBRs of 2.3 [42]. However, the superior binding characteristics of an antibody-based construct and the use of a brighter fluorophore (IRDye800CW vs. ICG) could potentially lead to higher absolute tumor signals for the monoclonal antibody compared to the peptide[7] [118, 122, 124]. Whether this is true can only be determined in a direct comparison between the various uPAR targeting tracers.

7 FluoGuide has recently started developing a variant of AE105 conjugated with IRDye800CW with the aim of improving the peptides TBR [124].

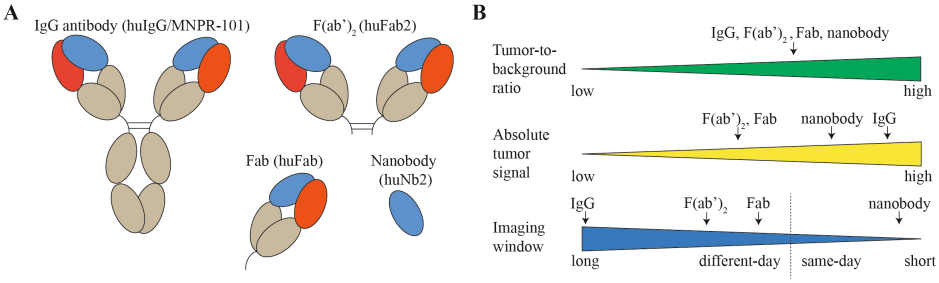

Figure 1. Comparison of various targeting FGS tracers. (A) Schematic representation of a IgG, F(ab')2, and Fab (B) Schematic representing differences in the outcomes tumor-to-background ratio, absolute tumor signal and imaging window between the different uPAR targeting tracers mentioned in this thesis. Peptide was not included on the absolute tumor signal scale as this cannot be reliably compared between different NIR-camera systems.

Conclusion

The field of uPAR research has come a long way since its initial discovery as a cell-based binding site for urokinase. Its role has greatly expanded from mere urokinase receptor to a central orchestrator of a multitude of pathways covering, amongst other things, cell proliferation, differentiation, and migration. While its intricacies are still being unraveled as we speak, its association with disease is undeniable. The immunohistochemical, in vivo and phase I/II clinical evidence gathered over the last two decades supports uPAR as a promising next generational target for FGS; in conclusion, the time is ripe for translating our preclinical knowledge of uPAR FGS to the clinic.

References

1. van Dam GM, Themelis G, Crane LM, Harlaar NJ, Pleijhuis RG, Kelder W, et al. Intraoperative tumor-specific fluorescence imaging in ovarian cancer by folate receptor-α targeting: first in-human results. Nat Med. 2011;17:1315-9. doi:10.1038/nm.2472.
2. Tanyi JL, Randall LM, Chambers SK, Butler KA, Winer IS, Langstraat CL, et al. A Phase III Study of Pafolacianine Injection (OTL38) for Intraoperative Imaging of Folate Receptor-Positive Ovarian Cancer (Study 006). Journal of clinical oncology : official journal of the American Society of Clinical Oncology. 2022:Jco2200291. doi:10.1200/jco.22.00291.
3. Hernot S, van Manen L, Debie P, Mieog JSD, Vahrmeijer AL. Latest developments in molecular tracers for fluorescence image-guided cancer surgery. The Lancet Oncology. 2019;20:e354-e67. doi:10.1016/s1470-2045(19)30317-1.
4. Eskander RN, Kauderer J, Tewari KS, Mannel RS, Bristow RE, O'Malley DM, et al. Correlation between Surgeon's assessment and radiographic evaluation of residual disease in women with advanced stage ovarian cancer reported to have undergone optimal surgical cytoreduction: An NRG Oncology/Gynecologic Oncology Group study. Gynecologic oncology. 2018;149:525-30. doi:10.1016/j.ygyno.2018.03.043.
5. Hoogstins CE, Tummers QR, Gaarenstroom KN, de Kroon CD, Trimbos JB, Bosse T, et al. A Novel Tumor-Specific Agent for Intraoperative Near-Infrared Fluorescence Imaging: A Translational Study in Healthy Volunteers and Patients with Ovarian Cancer. Clinical cancer research : an official journal of the American Association for Cancer Research. 2016;22:2929-38. doi:10.1158/1078-0432.Ccr-15-2640.
6. Tipirneni KE, Warram JM, Moore LS, Prince AC, de Boer E, Jani AH, et al. Oncologic Procedures Amenable to Fluorescence-guided Surgery. Annals of surgery. 2017;266:36-47. doi:10.1097/sla.0000000000002127.
7. Li MM, Puram SV, Silverman DA, Old MO, Rocco JW, Kang SY. Margin Analysis in Head and Neck Cancer: State of the Art and Future Directions. Annals of surgical oncology. 2019;26:4070-80. doi:10.1245/s10434-019-07645-9.
8. Stummer W, Pichlmeier U, Meinel T, Wiestler OD, Zanella F, Reulen HJ. Fluorescence-guided surgery with 5-aminolevulinic acid for resection of malignant glioma: a randomised controlled multicentre phase III trial. The Lancet Oncology. 2006;7:392-401. doi:10.1016/s1470-2045(06)70665-9.
9. van Gijn W, Marijnen CA, Nagtegaal ID, Kranenbarg EM, Putter H, Wiggers T, et al. Preoperative radiotherapy combined with total mesorectal excision for resectable rectal cancer: 12-year follow-up of the multicentre, randomised controlled TME trial. The Lancet Oncology. 2011;12:575-82. doi:10.1016/s1470-2045(11)70097-3.
10. Hoadley KA, Yau C, Hinoue T, Wolf DM, Lazar AJ, Drill E, et al. Cell-of-Origin Patterns Dominate the Molecular Classification of 10,000 Tumors from 33 Types of Cancer. Cell. 2018;173:291-304.e6. doi:10.1016/j.cell.2018.03.022.
11. Boonstra MC, de Geus SW, Prevoo HA, Hawinkels LJ, van de Velde CJ, Kuppen PJ, et al. Selecting Targets for Tumor Imaging: An Overview of Cancer-Associated Membrane Proteins. Biomarkers in cancer. 2016;8:119-33. doi:10.4137/bic.S38542.
12. Landercasper J, Whitacre E, Degnim AC, Al-Hamadani M. Reasons for re-excision after lumpectomy for breast cancer: insight from the American Society of Breast Surgeons Mastery(SM) database. Annals of surgical oncology. 2014;21:3185-91. doi:10.1245/s10434-014-3905-1.
13. Predina JD, Keating J, Patel N, Nims S, Singhal S. Clinical implications of positive margins following non-small cell lung cancer surgery. Journal of surgical oncology. 2016;113:264-9. doi:10.1002/jso.24130.

14. Schlick CJR, Khorfan R, Odell DD, Merkow RP, Bentrem DJ. Margin Positivity in Resectable Esophageal Cancer: Are there Modifiable Risk Factors? Annals of surgical oncology. 2020;27:1496-507. doi:10.1245/s10434-019-08176-z.
15. Fretland Å A, Dagenborg VJ, Bjørnelv GMW, Kazaryan AM, Kristiansen R, Fagerland MW, et al. Laparoscopic Versus Open Resection for Colorectal Liver Metastases: The OSLO-COMET Randomized Controlled Trial. Annals of surgery. 2018;267:199-207. doi:10.1097/sla.0000000000002353.
16. Allen VB, Gurusamy KS, Takwoingi Y, Kalia A, Davidson BR. Diagnostic accuracy of laparoscopy following computed tomography (CT) scanning for assessing the resectability with curative intent in pancreatic and periampullary cancer. The Cochrane database of systematic reviews. 2016;7:Cd009323. doi:10.1002/14651858.CD009323.pub3.
17. Lwin TM, Hoffman RM, Bouvet M. The development of fluorescence guided surgery for pancreatic cancer: from bench to clinic. Expert review of anticancer therapy. 2018;18:651-62. doi:10.1080/14737140.2018.1477593.
18. de Gooyer JM, Elekonawo FMK, Bremers AJA, Boerman OC, Aarntzen E, de Reuver PR, et al. Multimodal CEA-targeted fluorescence and radioguided cytoreductive surgery for peritoneal metastases of colorectal origin. Nature communications. 2022;13:2621. doi:10.1038/s41467-022-29630-9.
19. Yossepowitch O, Briganti A, Eastham JA, Epstein J, Graefen M, Montironi R, et al. Positive surgical margins after radical prostatectomy: a systematic review and contemporary update. European urology. 2014;65:303-13. doi:10.1016/j.eururo.2013.07.039.
20. van Rhijn BW, Burger M, Lotan Y, Solsona E, Stief CG, Sylvester RJ, et al. Recurrence and progression of disease in non-muscle-invasive bladder cancer: from epidemiology to treatment strategy. European urology. 2009;56:430-42. doi:10.1016/j.eururo.2009.06.028.
21. Dotan ZA, Kavanagh K, Yossepowitch O, Kaag M, Olgac S, Donat M, et al. Positive surgical margins in soft tissue following radical cystectomy for bladder cancer and cancer specific survival. J Urol. 2007;178:2308-12; discussion 13. doi:10.1016/j.juro.2007.08.023.
22. Ahn SB, Mohamedali A, Pascovici D, Adhikari S, Sharma S, Nice EC, et al. Proteomics Reveals Cell-Surface Urokinase Plasminogen Activator Receptor Expression Impacts Most Hallmarks of Cancer. Proteomics. 2019;19:e1900026. doi:10.1002/pmic.201900026.
23. Hanahan D. Hallmarks of Cancer: New Dimensions. Cancer Discov. 2022;12:31-46. doi:10.1158/2159-8290.Cd-21-1059.
24. Hanahan D, Weinberg RA. Hallmarks of cancer: the next generation. Cell. 2011;144:646-74. doi:10.1016/j.cell.2011.02.013.
25. Hanahan D, Weinberg RA. The hallmarks of cancer. Cell. 2000;100:57-70. doi:10.1016/s0092-8674(00)81683-9.
26. Saldanha RG, Xu N, Molloy MP, Veal DA, Baker MS. Differential proteome expression associated with urokinase plasminogen activator receptor (uPAR) suppression in malignant epithelial cancer. Journal of proteome research. 2008;7:4792-806. doi:10.1021/pr800357h.
27. Mahmood N, Mihalcioiu C, Rabbani SA. Multifaceted Role of the Urokinase-Type Plasminogen Activator (uPA) and Its Receptor (uPAR): Diagnostic, Prognostic, and Therapeutic Applications. Frontiers in oncology. 2018;8:24. doi:10.3389/fonc.2018.00024.
28. Smith HW, Marshall CJ. Regulation of cell signalling by uPAR. Nature reviews Molecular cell biology. 2010;11:23-36. doi:10.1038/nrm2821.
29. Boonstra MC, Verspaget HW, Ganesh S, Kubben FJ, Vahrmeijer AL, van de Velde CJ, et al. Clinical applications of the urokinase receptor (uPAR) for cancer patients. Current pharmaceutical design. 2011;17:1890-910. doi:10.2174/138161211796718233.

30. Leth JM, Ploug M. Targeting the Urokinase-Type Plasminogen Activator Receptor (uPAR) in Human Diseases With a View to Non-invasive Imaging and Therapeutic Intervention. Frontiers in cell and developmental biology. 2021;9:732015. doi:10.3389/fcell.2021.732015.
31. Fosbøl M, Kurbegovic S, Johannesen HH, Røder MA, Hansen AE, Mortensen J, et al. Urokinase-Type Plasminogen Activator Receptor (uPAR) PET/MRI of Prostate Cancer for Noninvasive Evaluation of Aggressiveness: Comparison with Gleason Score in a Prospective Phase 2 Clinical Trial. Journal of nuclear medicine : official publication, Society of Nuclear Medicine. 2021;62:354-9. doi:10.2967/jnumed.120.248120.
32. Carlsen EA, Loft M, Loft A, Berthelsen AK, Langer SW, Knigge U, et al. Prospective phase II trial of prognostication by (68)Ga-NOTA-AE105 uPAR PET in patients with neuroendocrine neoplasms: Implications for uPAR targeted therapy. Journal of nuclear medicine : official publication, Society of Nuclear Medicine. 2022. doi:10.2967/jnumed.121.263177.
33. Risør LM, Clausen MM, Ujmajuridze Z, Farhadi M, Andersen KF, Loft A, et al. Prognostic value of Urokinase-type Plasminogen Activator Receptor (uPAR)-PET/CT in Head and Neck Squamous Cell Carcinomas and Comparison with (18)F-FDG-PET/CT: A single-center prospective study. Journal of nuclear medicine : official publication, Society of Nuclear Medicine. 2021. doi:10.2967/jnumed.121.262866.
34. Fosbøl M, Mortensen J, Petersen PM, Loft A, Madsen J, Kjaer A. uPAR PET/CT for Prognostication and Response Assessment in Patients with Metastatic Castration-Resistant Prostate Cancer Undergoing Radium-223 Therapy: A Prospective Phase II Study. Diagnostics (Basel). 2021;11. doi:10.3390/diagnostics11061087.
35. Baart VM, Houvast RD, de Geus-Oei LF, Quax PHA, Kuppen PJK, Vahrmeijer AL, et al. Molecular imaging of the urokinase plasminogen activator receptor: opportunities beyond cancer. EJNMMI Res. 2020;10:87. doi:10.1186/s13550-020-00673-7.
36. Baart VM, van Duijn C, van Egmond SL, Dijckmeester WA, Jansen JC, Vahrmeijer AL, et al. EGFR and αvβ6 as Promising Targets for Molecular Imaging of Cutaneous and Mucosal Squamous Cell Carcinoma of the Head and Neck Region. Cancers (Basel). 2020;12. doi:10.3390/cancers12061474.
37. Christensen A, Grønhøj C, Jensen JS, Lelkaitis G, Kiss K, Juhl K, et al. Expression patterns of uPAR, TF and EGFR and their potential as targets for molecular imaging in oropharyngeal squamous cell carcinoma. Oncol Rep. 2022;48. doi:10.3892/or.2022.8359.
38. Hadjipanayis CG, Widhalm G, Stummer W. What is the Surgical Benefit of Utilizing 5-Aminolevulinic Acid for Fluorescence-Guided Surgery of Malignant Gliomas? Neurosurgery. 2015;77:663-73. doi:10.1227/neu.0000000000000929.
39. Gilder AS, Natali L, Van Dyk DM, Zalfa C, Banki MA, Pizzo DP, et al. The Urokinase Receptor Induces a Mesenchymal Gene Expression Signature in Glioblastoma Cells and Promotes Tumor Cell Survival in Neurospheres. Sci Rep. 2018;8:2982. doi:10.1038/s41598-018-21358-1.
40. Salajegheh M, Rudnicki A, Smith TW. Expression of urokinase-type plasminogen activator receptor (uPAR) in primary central nervous system neoplasms. Appl Immunohistochem Mol Morphol. 2005;13:184-9. doi:10.1097/01.pai.0000138448.85231.da.
41. Persson M, Nedergaard MK, Brandt-Larsen M, Skovgaard D, Jørgensen JT, Michaelsen SR, et al. Urokinase-Type Plasminogen Activator Receptor as a Potential PET Biomarker in Glioblastoma. Journal of nuclear medicine : official publication, Society of Nuclear Medicine. 2016;57:272-8. doi:10.2967/jnumed.115.161703.
42. FluoGuide. Presentation of FG001 results from the first clinical trial in aggressive brain cancer. youtube; 2022.

43. de Geus SW, Boogerd LS, Swijnenburg RJ, Mieog JS, Tummers WS, Prevoo HA, et al. Selecting Tumor-Specific Molecular Targets in Pancreatic Adenocarcinoma: Paving the Way for Image-Guided Pancreatic Surgery. Mol Imaging Biol. 2016;18:807-19. doi:10.1007/s11307-016-0959-4.
44. Tummers WS, Farina-Sarasqueta A, Boonstra MC, Prevoo HA, Sier CF, Mieog JS, et al. Selection of optimal molecular targets for tumor-specific imaging in pancreatic ductal adenocarcinoma. Oncotarget. 2017;8:56816-28. doi:10.18632/oncotarget.18232.
45. Rijs Z, Shifai AN, Bosma SE, Kuppen PJK, Vahrmeijer AL, Keereweer S, et al. Candidate Biomarkers for Specific Intraoperative Near-Infrared Imaging of Soft Tissue Sarcomas: A Systematic Review. Cancers (Basel). 2021;13. doi:10.3390/cancers13030557.
46. Linders D, Deken M, van der Valk M, Tummers W, Bhairosingh S, Schaap D, et al. CEA, EpCAM, αvβ6 and uPAR Expression in Rectal Cancer Patients with a Pathological Complete Response after Neoadjuvant Therapy. Diagnostics (Basel). 2021;11. doi:10.3390/diagnostics11030516.
47. Linders DGJ, Bijlstra OD, Fallert LC, Hilling DE, Walker E, Straight B, et al. Cysteine Cathepsins in Breast Cancer: Promising Targets for Fluorescence-Guided Surgery. Mol Imaging Biol. 2022. doi:10.1007/s11307-022-01768-4.
48. Houvast RD, Thijse K, Groen JV, Chua J, Vankemmelbeke M, Durrant LG, et al. An Immunohistochemical Evaluation of Tumor-Associated Glycans and Mucins as Targets for Molecular Imaging of Pancreatic Ductal Adenocarcinoma. Cancers (Basel). 2021;13. doi:10.3390/cancers13225777.
49. Ahn SB, Chan C, Dent OF, Mohamedali A, Kwun SY, Clarke C, et al. Epithelial and stromal cell urokinase plasminogen activator receptor expression differentially correlates with survival in rectal cancer stages B and C patients. PloS one. 2015;10:e0117786. doi:10.1371/journal.pone.0117786.
50. Serpa MS, Mafra RP, Queiroz S, Silva LPD, Souza LB, Pinto LP. Expression of urokinase-type plasminogen activator and its receptor in squamous cell carcinoma of the oral tongue. Braz Oral Res. 2018;32:e93. doi:10.1590/1807-3107bor-2018.vol32.0093.
51. Oh F, Modiano JF, Bachanova V, Vallera DA. Bispecific Targeting of EGFR and Urokinase Receptor (uPAR) Using Ligand-Targeted Toxins in Solid Tumors. Biomolecules. 2020;10. doi:10.3390/biom10060956.
52. Patil CG, Walker DG, Miller DM, Butte P, Morrison B, Kittle DS, et al. Phase 1 Safety, Pharmacokinetics, and Fluorescence Imaging Study of Tozuleristide (BLZ-100) in Adults With Newly Diagnosed or Recurrent Gliomas. Neurosurgery. 2019;85:E641-e9. doi:10.1093/neuros/nyz125.
53. Hatanpaa KJ, Burma S, Zhao D, Habib AA. Epidermal growth factor receptor in glioma: signal transduction, neuropathology, imaging, and radioresistance. Neoplasia. 2010;12:675-84. doi:10.1593/neo.10688.
54. Heimberger AB, Hlatky R, Suki D, Yang D, Weinberg J, Gilbert M, et al. Prognostic effect of epidermal growth factor receptor and EGFRvIII in glioblastoma multiforme patients. Clinical cancer research : an official journal of the American Association for Cancer Research. 2005;11:1462-6. doi:10.1158/1078-0432.Ccr-04-1737.
55. Bredel M, Pollack IF, Hamilton RL, James CD. Epidermal growth factor receptor expression and gene amplification in high-grade non-brainstem gliomas of childhood. Clinical cancer research : an official journal of the American Association for Cancer Research. 1999;5:1786-92.
56. Miller SE, Tummers WS, Teraphongphom N, van den Berg NS, Hasan A, Ertsey RD, et al. First-in-human intraoperative near-infrared fluorescence imaging of glioblastoma using cetuximab-IRDye800. J Neurooncol. 2018;139:135-43. doi:10.1007/s11060-018-2854-0.

57. Boonstra MC, Van Driel P, Keereweer S, Prevoo H, Stammes MA, Baart VM, et al. Preclinical uPAR-targeted multimodal imaging of locoregional oral cancer. Oral oncology. 2017;66:1-8. doi:10.1016/j.oraloncology.2016.12.026.
58. Ahmedah HT, Patterson LH, Shnyder SD, Sheldrake HM. RGD-Binding Integrins in Head and Neck Cancers. Cancers (Basel). 2017;9. doi:10.3390/cancers9060056.
59. de Geus SW, Baart VM, Boonstra MC, Kuppen PJ, Prevoo HA, Mazar AP, et al. Prognostic Impact of Urokinase Plasminogen Activator Receptor Expression in Pancreatic Cancer: Malignant Versus Stromal Cells. Biomark Insights. 2017;12:1177271917715443. doi:10.1177/1177271917715443.
60. Kenny HA, Leonhardt P, Ladanyi A, Yamada SD, Montag A, Im HK, et al. Targeting the urokinase plasminogen activator receptor inhibits ovarian cancer metastasis. Clinical cancer research : an official journal of the American Association for Cancer Research. 2011;17:459-71. doi:10.1158/1078-0432.Ccr-10-2258.
61. Markert S, Lassmann S, Gabriel B, Klar M, Werner M, Gitsch G, et al. Alpha-folate receptor expression in epithelial ovarian carcinoma and non-neoplastic ovarian tissue. Anticancer Res. 2008;28:3567-72.
62. Kalli KR, Oberg AL, Keeney GL, Christianson TJ, Low PS, Knutson KL, et al. Folate receptor alpha as a tumor target in epithelial ovarian cancer. Gynecologic oncology. 2008;108:619-26. doi:10.1016/j.ygyno.2007.11.020.
63. Tanyi JL, Chon HS, Morgan MA, Chambers SK, Han ES, Butler KA, et al. Phase 3, randomized, single-dose, open-label study to investigate the safety and efficacy of pafolacianine sodium injection (OTL38) for intraoperative imaging of folate receptor positive ovarian cancer. Journal of Clinical Oncology. 2021;39:5503-. doi:10.1200/JCO.2021.39.15_suppl.5503.
64. Spizzo G, Fong D, Wurm M, Ensinger C, Obrist P, Hofer C, et al. EpCAM expression in primary tumour tissues and metastases: an immunohistochemical analysis. Journal of clinical pathology. 2011;64:415-20. doi:10.1136/jcp.2011.090274.
65. Muynck L, Gaarenstroom KN, Sier CFM, Duijvenvoorde MV, Bosse T, Mieog JSD, et al. Novel Molecular Targets for Tumor-Specific Imaging of Epithelial Ovarian Cancer Metastases. Cancers (Basel). 2020;12. doi:10.3390/cancers12061562.
66. De Vos J, Devoogdt N, Lahoutte T, Muyldermans S. Camelid single-domain antibody-fragment engineering for (pre)clinical in vivo molecular imaging applications: adjusting the bullet to its target. Expert Opin Biol Ther. 2013;13:1149-60. doi:10.1517/14712598.2013.800478.
67. Cozzi PJ, Wang J, Delprado W, Madigan MC, Fairy S, Russell PJ, et al. Evaluation of urokinase plasminogen activator and its receptor in different grades of human prostate cancer. Hum Pathol. 2006;37:1442-51. doi:10.1016/j.humpath.2006.05.002.
68. Kumano M, Miyake H, Muramaki M, Furukawa J, Takenaka A, Fujisawa M. Expression of urokinase-type plasminogen activator system in prostate cancer: correlation with clinicopathological outcomes in patients undergoing radical prostatectomy. Urol Oncol. 2009;27:180-6. doi:10.1016/j.urolonc.2008.01.012.
69. Mannweiler S, Amersdorfer P, Trajanoski S, Terrett JA, King D, Mehes G. Heterogeneity of prostate-specific membrane antigen (PSMA) expression in prostate carcinoma with distant metastasis. Pathol Oncol Res. 2009;15:167-72. doi:10.1007/s12253-008-9104-2.
70. Bostwick DG, Pacelli A, Blute M, Roche P, Murphy GP. Prostate specific membrane antigen expression in prostatic intraepithelial neoplasia and adenocarcinoma: a study of 184 cases. Cancer. 1998;82:2256-61. doi:10.1002/(sici)1097-0142(19980601)82:11<2256::aid-cncr22>3.0.co;2-s.
71. Fendler WP, Eiber M, Beheshti M, Bomanji J, Ceci F, Cho S, et al. (68)Ga-PSMA PET/CT: Joint EANM and SNMMI procedure guideline for prostate cancer imaging: version 1.0. Eur J Nucl Med Mol Imaging. 2017;44:1014-24. doi:10.1007/s00259-017-3670-z.

72. Dohn LH, Pappot H, Iversen BR, Illemann M, Høyer-Hansen G, Christensen IJ, et al. uPAR Expression Pattern in Patients with Urothelial Carcinoma of the Bladder--Possible Clinical Implications. PloS one. 2015;10:e0135824. doi:10.1371/journal.pone.0135824.
73. Baart VM, van der Horst G, Deken MM, Bhairosingh SS, Schomann T, Sier VQ, et al. A multimodal molecular imaging approach targeting urokinase plasminogen activator receptor for the diagnosis, resection and surveillance of urothelial cell carcinoma. European journal of cancer (Oxford, England : 1990). 2021;146:11-20. doi:10.1016/j.ejca.2021.01.001.
74. Stenzl A, Burger M, Fradet Y, Mynderse LA, Soloway MS, Witjes JA, et al. Hexaminolevulinate guided fluorescence cystoscopy reduces recurrence in patients with nonmuscle invasive bladder cancer. J Urol. 2010;184:1907-13. doi:10.1016/j.juro.2010.06.148.
75. Khare HA, Døssing KBV, Ringgaard L, Christensen E, Urbak L, Sillesen H, et al. In vivo detection of urokinase-type plasminogen activator receptor (uPAR) expression in arterial atherogenesis using [(64)Cu]Cu-DOTA-AE105 positron emission tomography (PET). Atherosclerosis. 2022;352:103-11. doi:10.1016/j.atherosclerosis.2022.03.026.
76. Enocsson H, Lukic T, Ziegelasch M, Kastbom A. Serum levels of the soluble urokinase plasminogen activator receptor (suPAR) correlates with disease activity in early rheumatoid arthritis and reflects joint damage over time. Transl Res. 2021;232:142-9. doi:10.1016/j.trsl.2021.02.007.
77. Neijenhuis LKA, de Myunck L, Bijlstra OD, Kuppen PJK, Hilling DE, Borm FJ, et al. Near-Infrared Fluorescence Tumor-Targeted Imaging in Lung Cancer: A Systematic Review. Life (Basel). 2022;12. doi:10.3390/life12030446.
78. Predina JD, Newton AD, Connolly C, Dunbar A, Baldassari M, Deshpande C, et al. Identification of a Folate Receptor-Targeted Near-Infrared Molecular Contrast Agent to Localize Pulmonary Adenocarcinomas. Mol Ther. 2018;26:390-403. doi:10.1016/j.ymthe.2017.10.016.
79. Predina JD, Newton AD, Xia L, Corbett C, Connolly C, Shin M, et al. An open label trial of folate receptor-targeted intraoperative molecular imaging to localize pulmonary squamous cell carcinomas. Oncotarget. 2018;9:13517-29. doi:10.18632/oncotarget.24399.
80. Predina JD, Newton A, Corbett C, Xia L, Sulyok LF, Shin M, et al. Localization of Pulmonary Ground-Glass Opacities with Folate Receptor-Targeted Intraoperative Molecular Imaging. J Thorac Oncol. 2018;13:1028-36. doi:10.1016/j.jtho.2018.03.023.
81. Gangadharan S, Sarkaria IN, Rice D, Murthy S, Braun J, Kucharczuk J, et al. Multiinstitutional Phase 2 Clinical Trial of Intraoperative Molecular Imaging of Lung Cancer. Ann Thorac Surg. 2021;112:1150-9. doi:10.1016/j.athoracsur.2020.09.037.
82. Keating JJ, Runge JJ, Singhal S, Nims S, Venegas O, Durham AC, et al. Intraoperative near-infrared fluorescence imaging targeting folate receptors identifies lung cancer in a large-animal model. Cancer. 2017;123:1051-60. doi:10.1002/cncr.30419.
83. Azari F, Kennedy G, Bernstein E, Delikatny J, Lee JYK, Kucharczuk J, et al. Evaluation of OTL38-Generated Tumor-to-Background Ratio in Intraoperative Molecular Imaging-Guided Lung Cancer Resections. Mol Imaging Biol. 2021. doi:10.1007/s11307-021-01618-9.
84. Lanahan CR, Kelly BN, Gadd MA, Specht MC, Brown CL, Hughes KS, et al. Performance of a novel protease-activated fluorescent imaging system for intraoperative detection of residual breast cancer during breast conserving surgery. Breast cancer research and treatment. 2021;187:145-53. doi:10.1007/s10549-021-06106-w.
85. Smith BL, Lanahan CR, Specht MC, Kelly BN, Brown C, Strasfeld DB, et al. Feasibility Study of a Novel Protease-Activated Fluorescent Imaging System for Real-Time, Intraoperative Detection of Residual Breast Cancer in Breast Conserving Surgery. Annals of surgical oncology. 2020;27:1854-61. doi:10.1245/s10434-019-08158-1.

86. The American Society of Breast Surgeons Official Proceedings, Volume XXII 2021 Annual Meeting Scientific Session Abstracts. Annals of surgical oncology. 2021;28:163-400. doi:10.1245/s10434-021-10068-0.
87. de Gouw D, Rijpkema M, de Bitter TJJ, Baart VM, Sier CFM, Hernot S, et al. Identifying Biomarkers in Lymph Node Metastases of Esophageal Adenocarcinoma for Tumor-Targeted Imaging. Mol Diagn Ther. 2020;24:191-200. doi:10.1007/s40291-020-00448-9.
88. Went PT, Lugli A, Meier S, Bundi M, Mirlacher M, Sauter G, et al. Frequent EpCam protein expression in human carcinomas. Hum Pathol. 2004;35:122-8. doi:10.1016/j.humpath.2003.08.026.
89. van Manen L, Handgraaf HJM, Diana M, Dijkstra J, Ishizawa T, Vahrmeijer AL, et al. A practical guide for the use of indocyanine green and methylene blue in fluorescence-guided abdominal surgery. Journal of surgical oncology. 2018;118:283-300. doi:10.1002/jso.25105.
90. Boogerd LS, Handgraaf HJ, Lam HD, Huurman VA, Farina-Sarasqueta A, Frangioni JV, et al. Laparoscopic detection and resection of occult liver tumors of multiple cancer types using real-time near-infrared fluorescence guidance. Surg Endosc. 2017;31:952-61. doi:10.1007/s00464-016-5007-6.
91. Achterberg FB, Sibinga Mulder BG, Meijer RPJ, Bonsing BA, Hartgrink HH, Mieog JSD, et al. Real-time surgical margin assessment using ICG-fluorescence during laparoscopic and robot-assisted resections of colorectal liver metastases. Ann Transl Med. 2020;8:1448. doi:10.21037/atm-20-1999.
92. Meijer RPJ, de Valk KS, Deken MM, Boogerd LSF, Hoogstins CES, Bhairosingh SS, et al. Intraoperative detection of colorectal and pancreatic liver metastases using SGM-101, a fluorescent antibody targeting CEA. Eur J Surg Oncol. 2021;47:667-73. doi:10.1016/j.ejso.2020.10.034.
93. Tiernan JP, Perry SL, Verghese ET, West NP, Yeluri S, Jayne DG, et al. Carcinoembryonic antigen is the preferred biomarker for in vivo colorectal cancer targeting. Br J Cancer. 2013;108:662-7. doi:10.1038/bjc.2012.605.
94. Boogerd LS, van der Valk MJ, Boonstra MC, Prevoo HA, Hilling DE, van de Velde CJ, et al. Biomarker expression in rectal cancer tissue before and after neoadjuvant therapy. Onco Targets Ther. 2018;11:1655-64. doi:10.2147/ott.S145473.
95. Went P, Vasei M, Bubendorf L, Terracciano L, Tornillo L, Riede U, et al. Frequent high-level expression of the immunotherapeutic target Ep-CAM in colon, stomach, prostate and lung cancers. Br J Cancer. 2006;94:128-35. doi:10.1038/sj.bjc.6602924.
96. Schmelzer E, Reid LM. EpCAM expression in normal, non-pathological tissues. Front Biosci. 2008;13:3096-100. doi:10.2741/2911.
97. Schmidt MM, Wittrup KD. A modeling analysis of the effects of molecular size and binding affinity on tumor targeting. Mol Cancer Ther. 2009;8:2861-71. doi:10.1158/1535-7163.Mct-09-0195.
98. Thurber GM, Schmidt MM, Wittrup KD. Antibody tumor penetration: transport opposed by systemic and antigen-mediated clearance. Adv Drug Deliv Rev. 2008;60:1421-34. doi:10.1016/j.addr.2008.04.012.
99. Xenaki KT, Oliveira S, van Bergen En Henegouwen PMP. Antibody or Antibody Fragments: Implications for Molecular Imaging and Targeted Therapy of Solid Tumors. Front Immunol. 2017;8:1287. doi:10.3389/fimmu.2017.01287.
100. Baart VM, van Manen L, Bhairosingh SS, Vuijk FA, Iamele L, de Jonge H, et al. Side-by-Side Comparison of uPAR-Targeting Optical Imaging Antibodies and Antibody Fragments for Fluorescence-Guided Surgery of Solid Tumors. Mol Imaging Biol. 2021. doi:10.1007/s11307-021-01657-2.

101. Hong H, Zhang Y, Orbay H, Valdovinos HF, Nayak TR, Bean J, et al. Positron emission tomography imaging of tumor angiogenesis with a (61/64)Cu-labeled F(ab')(2) antibody fragment. Mol Pharm. 2013;10:709-16. doi:10.1021/mp300507r.
102. Zhang Y, Hong H, Orbay H, Valdovinos HF, Nayak TR, Theuer CP, et al. PET imaging of CD105/endoglin expression with a $^{61}/^{64}$Cu-labeled Fab antibody fragment. Eur J Nucl Med Mol Imaging. 2013;40:759-67. doi:10.1007/s00259-012-2334-2.
103. El-Sayed A, Bernhard W, Barreto K, Gonzalez C, Hill W, Pastushok L, et al. Evaluation of antibody fragment properties for near-infrared fluorescence imaging of HER3-positive cancer xenografts. Theranostics. 2018;8:4856-69. doi:10.7150/thno.24252.
104. Li D, Liu S, Liu R, Zhou Y, Park R, Naga K, et al. EphB4-targeted imaging with antibody h131, h131-F(ab')2 and h131-Fab. Mol Pharm. 2013;10:4527-33. doi:10.1021/mp400354y.
105. Leelawattanachai J, Kwon KW, Michael P, Ting R, Kim JY, Jin MM. Side-by-Side Comparison of Commonly Used Biomolecules That Differ in Size and Affinity on Tumor Uptake and Internalization. PloS one. 2015;10:e0124440. doi:10.1371/journal.pone.0124440.
106. Thurber GM, Zajic SC, Wittrup KD. Theoretic criteria for antibody penetration into solid tumors and micrometastases. Journal of nuclear medicine : official publication, Society of Nuclear Medicine. 2007;48:995-9. doi:10.2967/jnumed.106.037069.
107. Wittrup KD, Thurber GM, Schmidt MM, Rhoden JJ. Practical theoretic guidance for the design of tumor-targeting agents. Methods Enzymol. 2012;503:255-68. doi:10.1016/b978-0-12-396962-0.00010-0.
108. Tang Y, Lou J, Alpaugh RK, Robinson MK, Marks JD, Weiner LM. Regulation of antibody-dependent cellular cytotoxicity by IgG intrinsic and apparent affinity for target antigen. Journal of immunology (Baltimore, Md : 1950). 2007;179:2815-23. doi:10.4049/jimmunol.179.5.2815.
109. Graff CP, Wittrup KD. Theoretical analysis of antibody targeting of tumor spheroids: importance of dosage for penetration, and affinity for retention. Cancer Res. 2003;63:1288-96.
110. Adams GP, Schier R, Marshall K, Wolf EJ, McCall AM, Marks JD, et al. Increased affinity leads to improved selective tumor delivery of single-chain Fv antibodies. Cancer Res. 1998;58:485-90.
111. Zahnd C, Kawe M, Stumpp MT, de Pasquale C, Tamaskovic R, Nagy-Davidescu G, et al. Efficient tumor targeting with high-affinity designed ankyrin repeat proteins: effects of affinity and molecular size. Cancer Res. 2010;70:1595-605. doi:10.1158/0008-5472.Can-09-2724.
112. Rudnick SI, Lou J, Shaller CC, Tang Y, Klein-Szanto AJ, Weiner LM, et al. Influence of affinity and antigen internalization on the uptake and penetration of Anti-HER2 antibodies in solid tumors. Cancer Res. 2011;71:2250-9. doi:10.1158/0008-5472.Can-10-2277.
113. Sadiki A, Vaidya SR, Abdollahi M, Bhardwaj G, Dolan ME, Turna H, et al. Site-specific conjugation of native antibody. Antib Ther. 2020;3:271-84. doi:10.1093/abt/tbaa027.
114. Cohen R, Stammes MA, de Roos IH, Stigter-van Walsum M, Visser GW, van Dongen GA. Inert coupling of IRDye800CW to monoclonal antibodies for clinical optical imaging of tumor targets. EJNMMI Res. 2011;1:31. doi:10.1186/2191-219x-1-31.
115. Conner KP, Rock BM, Kwon GK, Balthasar JP, Abuqayyas L, Wienkers LC, et al. Evaluation of near infrared fluorescent labeling of monoclonal antibodies as a tool for tissue distribution. Drug Metab Dispos. 2014;42:1906-13. doi:10.1124/dmd.114.060319.
116. Cilliers C, Nessler I, Christodolu N, Thurber GM. Tracking Antibody Distribution with Near-Infrared Fluorescent Dyes: Impact of Dye Structure and Degree of Labeling on Plasma Clearance. Mol Pharm. 2017;14:1623-33. doi:10.1021/acs.molpharmaceut.6b01091.

117. Debie P, Van Quathem J, Hansen I, Bala G, Massa S, Devoogdt N, et al. Effect of Dye and Conjugation Chemistry on the Biodistribution Profile of Near-Infrared-Labeled Nanobodies as Tracers for Image-Guided Surgery. Mol Pharm. 2017;14:1145-53. doi:10.1021/acs.molpharmaceut.6b01053.
118. Kurbegovic S, Juhl K, Chen H, Qu C, Ding B, Leth JM, et al. Molecular Targeted NIR-II Probe for Image-Guided Brain Tumor Surgery. Bioconjugate chemistry. 2018;29:3833-40. doi:10.1021/acs.bioconjchem.8b00669.
119. Keyaerts M, Xavier C, Heemskerk J, Devoogdt N, Everaert H, Ackaert C, et al. Phase I Study of 68Ga-HER2-Nanobody for PET/CT Assessment of HER2 Expression in Breast Carcinoma. Journal of nuclear medicine : official publication, Society of Nuclear Medicine. 2016;57:27-33. doi:10.2967/jnumed.115.162024.
120. Boogerd LSF, Hoogstins CES, Schaap DP, Kusters M, Handgraaf HJM, van der Valk MJM, et al. Safety and effectiveness of SGM-101, a fluorescent antibody targeting carcinoembryonic antigen, for intraoperative detection of colorectal cancer: a dose-escalation pilot study. The lancet Gastroenterology & hepatology. 2018;3:181-91. doi:10.1016/s2468-1253(17)30395-3.
121. de Valk KS, Deken MM, Schaap DP, Meijer RP, Boogerd LS, Hoogstins CE, et al. Dose-Finding Study of a CEA-Targeting Agent, SGM-101, for Intraoperative Fluorescence Imaging of Colorectal Cancer. Annals of surgical oncology. 2021;28:1832-44. doi:10.1245/s10434-020-09069-2.
122. Baart VM, Boonstra MC, Sier CFM. uPAR directed-imaging of head-and-neck cancer. Oncotarget. 2017;8:20519-20. doi:10.18632/oncotarget.16240.
123. Galema HA, Meijer RPJ, Lauwerends LJ, Verhoef C, Burggraaf J, Vahrmeijer AL, et al. Fluorescence-guided surgery in colorectal cancer; A review on clinical results and future perspectives. Eur J Surg Oncol. 2022;48:810-21. doi:10.1016/j.ejso.2021.10.005.
124. Gioux S, Choi HS, Frangioni JV. Image-guided surgery using invisible near-infrared light: fundamentals of clinical translation. Molecular imaging. 2010;9:237-55.